Scientific Research Publishing

Journal of Modern Physics, 2023, 14, 1641-1661
https://www.scirp.org/journal/jmp
ISSN Online: 2153-120X
ISSN Print: 2153-1196

Dark Matter, Dark Energy, and Occam's Razor

J. C. Botke

Ronin Institute, Montclair, NJ, USA
Email: jcbotke(at)ronininstitute.org

How to cite this paper: Botke, J.C. (2023) Dark Matter, Dark Energy, and Occam's Razor. *Journal of Modern Physics*, **14**, 1641-1661.
https://doi.org/10.4236/jmp.2023.1412096

Received: October 24, 2023
Accepted: November 25, 2023
Published: November 28, 2023

Abstract

Even though dark matter and dark energy have long been accepted as being of fundamental importance in cosmology, in this paper, we will present arguments to show that neither is necessary. Instead, the phenomena they are thought to be responsible for are consequences of a vacuum whose curvature varies with time. We will focus on three phenomena that are thought to require the existence of dark energy and dark matter. The first is the idea that dark energy is responsible for the observed accelerating expansion of the universe. We will show instead that with time-varying curvature, Einstein's equations demand such an acceleration without reference to dark or any other form of energy. Turning to dark matter, it is supposedly required to explain the observed constant velocity profile of the stars making up the disks of spiral galaxies and to explain the strong gravitational lensing observed in galaxy clusters. We will show, however, that both phenomena can again be understood in terms of the vacuum and its curvature. In the former case, we will show that galaxies exist within a rotating volume of the vacuum and that this leads directly to the observed constant velocity profiles. In the latter case, gradients of the vacuum curvature serving as a varying index of refraction are responsible. Using numerical results from our new model of nucleosynthesis, we estimate the degree of bending to expect and find that the results are in accord with observation. Our new model very naturally explains the phenomena attributed to dark matter and dark energy and since neither has been observed after several decades of looking, Occam's razor tells us that neither exists.

Keywords

Dark Matter, Dark Energy, Early Universe, Accelerated Expansion, Gravitational Lensing, Evolution of the Universe

1. Introduction

In this paper, we will show that the phenomena commonly attributed to dark

matter and dark energy are instead consequences of the spacetime vacuum and its curvature. Our conclusions follow from our new model of cosmology which is based on the idea that the curvature of the vacuum varies with time and that the energy density and curvature are opposite sides of the same coin [1] [2]. The three phenomena that we will be discussing include the accelerating expansion of the universe, the constant velocity profiles of spiral galaxies, and strong gravitational lensing of galaxy clusters. Each of these can be understood in terms of different aspects of the vacuum. The accelerating expansion, which is the sole bases for the dark energy idea, is shown to be a kinematic effect resulting from the time variation of the vacuum curvature. The constant velocity profiles are shown to be a relativistic effect that follows from the coupling of the rotation of matter with that of the vacuum, and gravitational lensing is shown to be a consequence of variations in the vacuum energy density and hence, its curvature within galaxy clusters.

In the spiral galaxy case, we will show that all galaxies exist within a rotating volume of the vacuum which is coupled to the ordinary matter of the galaxy by a process akin to inertial frame dragging. The consequence is that the stars in the outer regions of the galaxies are actually at rest in a vacuum rotating as a rigid body, and this leads directly to the observed constant velocity profile.

Referring next to gravitational lensing, spatial variations in the vacuum curvature cause changes in the travel time of photons between any two points so in more familiar terms, the vacuum constitutes a medium with a varying index of refraction. One significant difference between this and the dark matter model is that refraction depends on small gradients in the curvature and not on its magnitude. Thus, unlike the large mass required by the dark matter model, there is no need for large vacuum energy densities and in fact, the vacuum energy density within clusters is only a few percent of the average ordinary matter energy density.

To understand these issues, it is necessary to have some idea of the structure of this new model so we will present a synopsis. A more detailed summary is given in [1] for those interested. According to this model, the universe came into existence with a Planck-era inflation during which there was no existence other than the vacuum, and time and distance were uncertain. Because the largest present-day cosmic structures are too large to have been the consequence of any causal process, it must have been during that epoch that they, along with everything else, were defined. The definition took the form of acausal vacuum energy density structures or imprints that then came into existence, and that later regulated the formation of ordinary matter. That event, which began at a time of about 10^{-5} s, marked the beginning of nucleosynthesis. The initial phase of nucleosynthesis lasted about 10^{-12} s, [3] and resulted in the creation of a high density of neutrons and protons and much higher densities of photons (that became the cosmic microwave background (CMB)), pions, and leptons. During the intermezzo that followed, the radiation became blackbody and the proton-neutron

ratio was adjusted by weak interactions from an initial value of $p:n=1:1$ to its final value of $p:n=7:1$.

Following this phase which ended at a time of about 1 second, protons and neutrons collisions initiated a series of inelastic nuclear reactions that created the initial populations of the light elements. At the conclusion of this process, the material content of the universe consisted primarily of protons with a small percentage of helium and trace amounts of other light elements.

The resulting densities of matter varied from place to place in conformity to the vacuum imprint. Regions with higher densities became the cosmic structures from stars on up to the cosmic web and those with lower densities became cosmic voids. In [4], we follow the subsequent evolution of these proto-structures to show that they all came into their fully developed final form more or less simultaneously at a time of about 1×10^{16} s, and in [5], we show that the stability of galaxies and galaxy clusters required that all galaxies formed supermassive black holes at that time. We contrast this with the prevailing view of galaxy formation based on accretion which predicts that galaxies should have been initially been fragmentary and only later achieved their final form. We now have the evidence coming from the James Webb telescope which supports our new model rather than the old accretion model of galaxy formation.

With that, we will turn to the dark energy problem.

2. The Reality of Dark Energy

In this section, we will show that a universe with time-varying curvature must exhibit a present-day exponential accelerated expansion that is not connected with dark or any other form of energy. Our argument follows from a new solution of Einstein's equations [2], so we will begin with a discussion to motivate our choice of metric.

In common with the standard model, we envision a universe consisting of a sequence of hyperspheres that are homogeneous and isotropic but that is as far as the common ground goes. In the standard model, the additional assumption is made that the universe must *appear* homogeneous and isotropic and for that to happen, the curvature must not vary with time. We instead assert that the curvature does vary with time. The consequence is that, while the universe is homogeneous and isotropic on each hypersphere, each has a different curvature so the universe will not appear homogeneous and isotropic. Signals detected by an observer will have experienced a range of curvatures as they proceed from sources to the observer and the result will depend on the location of the sources[1].

To proceed, we need to develop the equations that describe the evolution of

[1]Our new model has been criticized because it appears to violate the so-called cosmological principle but the latter has no precise definition and without a definition, it is not possible to say whether some variation of curvature is in violation or not. There is also the point that homogeneous and isotropic as used in cosmological models applies only to the background vacuum which is not directly observable. The CMB anisotropy spectrum, on the other hand, shows that distribution of the ordinary matter is neither homogeneous nor isotropic on any distance scale so the cosmological principle is an empty concept that serves no useful purpose.

the hyperspheres or, in other words, their scaling and curvature, and for that, we need to formulate a metric that reflects these ideas. The problem is that hyperspheres have no notion of a preferred origin and their properties are dependent only on (cosmic) time. Each point of a hypersphere is equivalent to every other point and all distances are space-like. Einstein's equations, on the other hand, are time-like and it is not possible to get anywhere with them without specifying an origin. The question then, is how do we reconcile Einstein's equations which describe our perceptions with a sequence of hyperspheres that have no notion of an origin? The answer is that Einstein's equations describe the universe as viewed by each observer from the viewpoint of an origin at the observer's location. But a hypersphere is simply the collection of all possible observer origins so Einstein's equations become the equations that describe the hypersphere *when evaluated at any observer's origin*. Said another way, separations on a hypersphere are space-like and since Einstein's equations only describe time-like events, the only point of contact is with a signal of zero spatial extent. This means that Einstein's equations describe hyperspheres in the limit that the radial coordinate goes to zero. (Note that the Freedman-Robertson-Walker (FRW) equations gloss over this point because they don't depend on the radial coordinate.)

A review of the development of the FRW metric will show that each hypersphere must have a uniform curvature if the hypersphere is to exhibit homogeneity and isotropy. The idea that all hyperspheres should have the *same* uniform curvature is a separate idea which we assert is not the case in the actual universe. To have homogeneous and isotropic hyperspheres, our metric must look something like the FRW metric but with time-varying curvature, $k = k(ct)$. With that change, we find that the metric must also contain an off-diagonal term connecting time with distance and a time-dependent factor in the coefficient of $(c\mathrm{d}t)^2$. These together embody the idea that the universe will not appear homogenous and isotropic to an observer. Putting these ideas together, the metric becomes

$$\begin{aligned} \mathrm{d}s^2 = &\left(-1 + \frac{r^2 h(ct,r)^2}{a(ct)^2}\left(1 - k(ct) r^2\right)\right)(c\mathrm{d}t)^2 \\ &+ 2h(ct,r)(cdt) r\mathrm{d}r + a^2(ct)\left(\frac{\mathrm{d}r^2}{1-k(ct)r^2} + r^2 \mathrm{d}\Omega^2\right) \end{aligned} \tag{2.1}$$

In this metric, r is the radial coordinate which varies from 0 to 1, $k(ct)$ is the time-varying curvature, $a(ct)$ is the scaling of the universe, and $h(ct,r)$ is a measure of the degree to which the time and radial coordinates are coupled as a result of the time variation of the curvature.

We also must specify the energy-momentum tensor. The standard model concept of a vacuum is

$$\boldsymbol{T}^{\mu\nu} = 0 \tag{2.2}$$

and while this is appropriate for dense objects such as stars where the energy

density is much greater than that of the vacuum, it is not appropriate when considering the vacuum alone. Including the vacuum energy results in the following energy-momentum tensor,

$$\boldsymbol{T}^{\mu\nu} = \left(\rho_{vac}c^2\left(ct,r\right) + p_{vac}\left(ct,r\right)\right)\delta_0^\mu\delta_0^\nu + p_{vac}\left(ct,r\right)\boldsymbol{g}^{\mu\nu} \tag{2.3}$$

where ρ_{vac} and p_{vac} are the energy density and pressure of the vacuum respectively. As we will see, this results in the curvature acting as its own source. After working out Einstein's equations (using Mathematica) and taking the limit $r \to 0$, the resulting equations can be solved in closed form. The scaling is given by,

$$a\left(ct\right) = a_*\left(\frac{ct}{ct_0}\right)^{\gamma_*} \mathrm{e}^{\frac{ct}{ct_0}c_1} \tag{2.4}$$

where

$$a_* = a_0\mathrm{e}^{-c_1}. \tag{2.5}$$

We see that the scaling is power-law for $ct/ct_0 \ll 1$ and exponential for $ct/ct_0 \geq 1$. The curvature is given by

$$k\left(ct\right) = k_0\left(\frac{a\left(ct\right)}{a\left(ct_0\right)}\frac{ct_0}{ct}\right)^2 \tag{2.6}$$

which is related to the vacuum energy density and pressure by

$$k\left(ct\right) = \frac{1}{2}\gamma_h a\left(ct\right)^2\kappa\left(\rho_{vac}c^2\left(ct,0\right) + p_{vac}\left(ct,0\right)\right). \tag{2.7}$$

We see from this that the curvature is determined by the energy density of the vacuum but the energy density of the vacuum is contained in its curvature so the curvature is acting as its own source.

The energy-pressure sum is thus a fixed function of time,

$$\rho_{vac}c^2\left(ct,0\right) + p_{vac}\left(ct,0\right) = \frac{2k_0}{\kappa a_0^2\gamma_h}\frac{\left(ct_0\right)^2}{\left(ct\right)^2} \tag{2.8}$$

As part of the solution, we find that both the energy density and the pressure contain a constant term that one might think to associate with a cosmological constant. These terms, however, have no physical consequences, and in fact, they can be removed by simply adding a constant term to the energy-momentum tensor. The curvature is a function of the sum rather than either energy or pressure individually and in the sum, the constant terms cancel.

Aside from the present-day size and age of the universe, to fix the parameters of the model, we need the value of the scaling at two different times. For one, we use the present-day value of the Hubble constant. There is some uncertainty about its value but a value of $H_0 = 73\,\mathrm{km}/\left(\mathrm{s}\cdot\mathrm{Mpc}\right)$ is emerging from the various methods used to measure its value. Although we don't show the results here, in support of our new model, its prediction of the supernovae luminosity distance precisely matches the best fit obtained by the SHOES observation group,

[6].

For the other parameter, we use the energy density of the CMB at the time of nucleosynthesis. From this, we determine that γ_* can be at most only slightly greater than 1/2. We needed to choose a single value and have found that a value of exactly 1/2 gives reasonable results. The Hubble parameter is by definition $H(ct) \equiv \dot{a}(ct)/a(ct)$. After substituting Equation (2.4), we find $c_1 = t_0 H_0 - \gamma_*$ where H_0 is the present-day value of the Hubble constant. The parameter c_1 always has a value close to 1/2 and for $H_0 = 73$, $c_1 = 0.53$.

There appears to be one remaining parameter, namely the present-day value of the curvature, k_0. During and shortly after the inflation, the curvature was maximal which motivates an additional principle that states that the *curvature must always be as large as possible* or equivalently, that the vacuum energy density *must always be as large as possible*. The value $k_0 = 1.414$ follows from the solution of equations outlined above. The details of the derivation, which are too lengthy to present here, are given in [2].

Everything is now fixed and unambiguous predictions can be made. This situation is completely different from that of the standard FRW model because the latter does not predict anything based solely on its being a solution to the equations. By making choices about various parameters, it is possible to predict any sort of evolution one cares to see. In the new model that is not the case. There is one solution, there are no free parameters, and *only one evolution is possible*.

We will now show some predictions of the model. These don't all have a direct bearing on the dark energy issue but they will give the reader a better idea of the universe described by the new model. We define an effective scaling parameter $a(t) = a_0 e^{\gamma_{eff}(t)}$ which we show in **Figure 1**. The exponential acceleration of the scaling is clearly visible. We also show the scaling as a function of time.

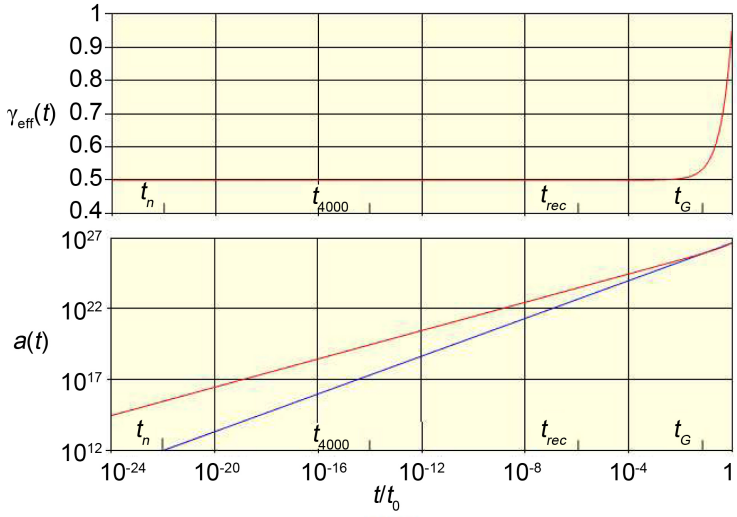

Figure 1. Time-varying curvature predictions are shown in red. For comparison, the curve for $2/3^{rds}$ scaling is shown in blue. The indicated times are t_n = the beginning of nucleosynthesis, t_{4000} = the end of nucleosynthesis, t_{rec} = the time of recombination, and t_G = galaxy formation.

In Figure 2, we show the coordinate distance of sources whose signals are received at present plotted as a function of the look-back time. Both time-varying and constant curvature cases are shown. The two curves are similar for small values of look-back time but differ considerably for large redshifts which illustrates our point about the universe only appearing inhomogeneous and anisotropic for large redshifts. Note that with time-varying curvature, there is a fundamental limitation on our ability to detect distance sources. No matter how far back in time we look, we cannot see sources with coordinate distances greater than about $r = 0.6$. The reason for this is that the proper path length for a photon increases with increasing curvature and eventually, the curvature becomes so large that the distance to the source becomes infinite.

The redshift is shown in Figure 3.

In Figure 4 and Figure 5, we show the curvature as a function of both the look-back time and redshift. From these two figures, we see that the curvature doesn't vary significantly until we are back to about half the present age of the universe.

Finally, in Figure 6, we show the coordinate distance as a function of the redshift. Again, we see the coordinate distance of observable objects approaching a limiting value for large redshifts.

We already established our main point concerning the reality of dark energy when we presented the solution for the scaling in Equation (2.4). It is interesting,

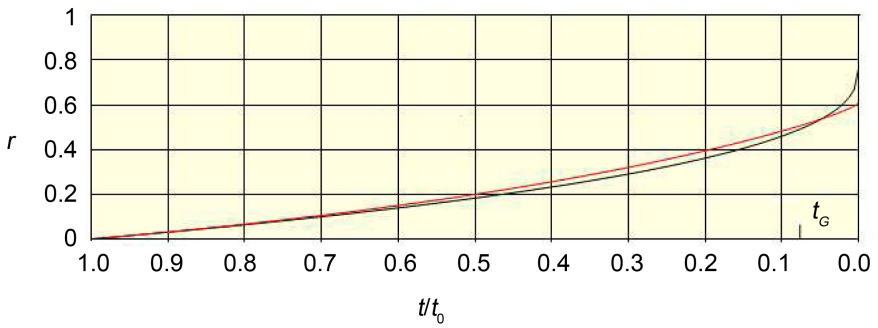

Figure 2. Coordinate distance r vs look-back time. The red curve is the time-varying curvature result. For comparison, in black, we also show the result computed assuming a constant value of $k = 1$.

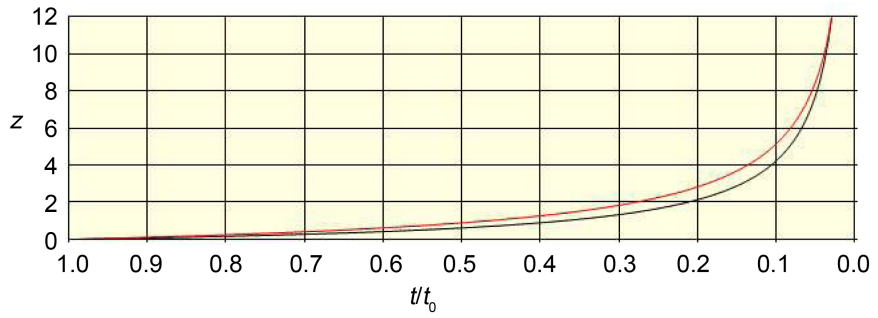

Figure 3. Redshift vs look-back time. The time-varying curvature result is shown in red and the $k = 1$ result is shown in black.

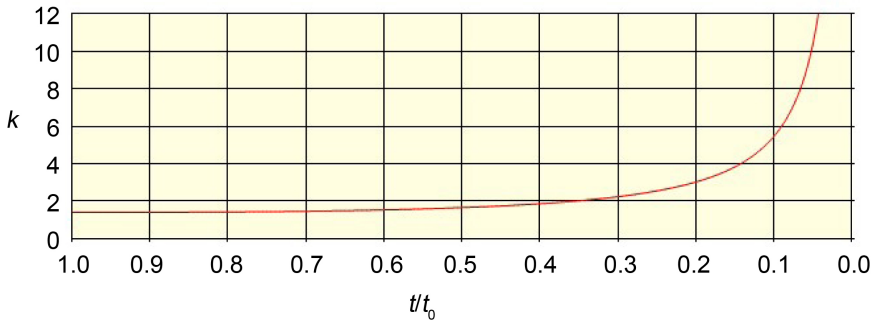

Figure 4. Curvature as a function of time.

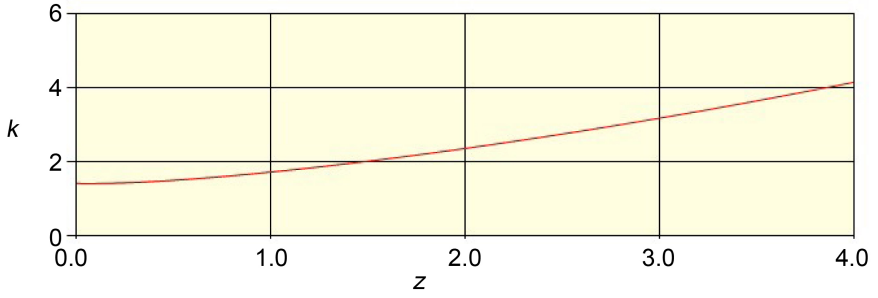

Figure 5. Curvature as a function of redshift.

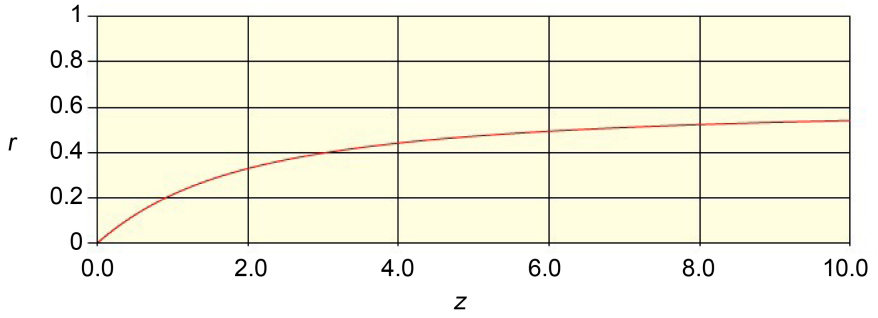

Figure 6. Coordinate distance as a function of redshift.

however, to compare the dark energy value with that of the vacuum energy density. From Equation (2.8), we find that the present-day vacuum energy density is

$$\rho_{vac}c^2\left(ct_0,0\right)+p_{vac}\left(ct_0,0\right)=2.1\times10^{-10}\ \mathrm{j}\cdot\mathrm{m}^{-3} \tag{2.9}$$

This differs from the generally accepted value of the dark energy density (6.3×10^{-10} jm^{-3}) by no more than a factor of 3. This value is also very close to the present-day energy density of all the ordinary matter in the universe which is about 1.5×10^{-10} jm^{-3}.

Even though the magnitudes of the vacuum energy and dark energy are similar, the two are in no way equivalent. From the equations, we see that there is no direct relationship between the scaling and the energy density or pressure. The present-day acceleration of the scaling is, in fact, a kinematic constraint that follows directly from the time variation of the curvature and the presence of the vacuum energy in the energy-momentum tensor. The fact that our new model

predicts an accelerating expansion proves that there is no need for dark energy to explain the phenomenon and since that is the only reason for presuming its existence, there is no reason to continue to believe that dark energy exists.

In the next section, we will take up the first of the dark matter issues, namely the spiral galaxy velocity problem.

3. Spiral Galaxy Velocity Problem

The spiral galaxy velocity problem is illustrated by the curves in Figure 7. (The same behavior is also seen in the velocity distribution of the gases making up the large HI rings that surround some galaxies, particularly lenticular galaxies [7]).

The problem is that the observed distribution, curve B does not match the expected distribution based on normal orbital motions, curve A. An example of an actual velocity profile is given in [8]. The generally accepted solution for this problem has been to suppose that there is a halo of dark matter surrounding the galaxy which provides the gravitation needed to match the observed velocity distribution. To get a hint about an alternate solution, we subtract the two curves to obtain curve C and notice that it approximates the velocity profile of a rotating rigid body. This suggests that the observed velocity distribution of the stars can be understood in terms of some normal orbital motion riding along inside a rigidly rotating background.

We need a model to study this problem and given the symmetry of spiral galaxies, it is reasonable to assume a stationary axisymmetric metric.

$$\mathrm{d}s^2 = -\left(A - \frac{B\omega^2}{c^2}\right)(c\mathrm{d}t)^2 - 2\frac{B\omega}{c}\mathrm{d}\psi(c\mathrm{d}t) + B\mathrm{d}\varphi^2 + C\mathrm{d}r^2 + D\mathrm{d}\psi^2 \tag{3.1}$$

The energy-momentum tensor must include both the vacuum and the ordinary matter making up the galaxy so, with the assumption that the matter does not exert pressure. it has the form

$$\boldsymbol{T}^{\mu\nu} = \left(\rho_{vac}c^2 + p_{vac}\right)\frac{u^\mu u^\nu}{c^2} + p_{vac}\boldsymbol{g}^{\mu\nu} + \rho_m c^2\frac{v^\mu v^\nu}{c^2} \tag{3.2}$$

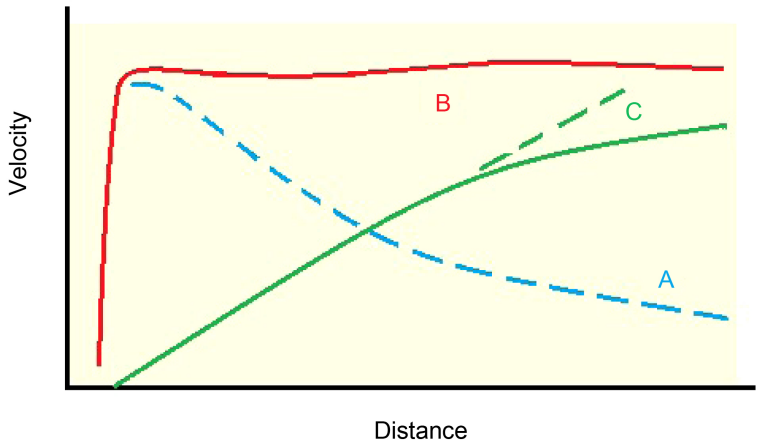

Figure 7. Typical spiral galactic velocity distribution.

The arguments of all the functions have been suppressed for brevity. The vacuum quantities are denoted by the subscript "*vac*" and the matter by the subscript "*m*". The angle ψ is defined by $\psi = \frac{\pi}{2} - \theta$ where θ is the usual spherical coordinates polar angle. With this definition, $\psi = 0$ defines the plane of the galaxy. It would be nice to be able to solve the full set of Einstein's equations for the metric functions given the boundary condition that the solution must match the background vacuum solution of Section 2 at large distances but that turns out to be a formidable problem requiring a finite element analysis on a supercomputer. Since we don't have such access, we must make do with less. Fortunately, we can make quite a bit of progress towards understanding the general structure of the solution through consideration of the much simpler geodetic equations.

A small volume of the vacuum will respond to the total gravitation field in the same way as a material particle which means that we can analyze its motion using the usual geodesic equations.

$$\begin{aligned}
\frac{\mathrm{d}u^0}{\mathrm{d}t} &= \Gamma^0_{00}u^0u^0 + 2\Gamma^0_{01}u^0u^1 + \Gamma^0_{11}u^1u^1 = 0 \\
\frac{\mathrm{d}u^1}{\mathrm{d}t} &= \Gamma^1_{00}u^0u^0 + 2\Gamma^1_{01}u^0u^1 + \Gamma^1_{11}u^1u^1 = 0 \\
\frac{\mathrm{d}u^2}{\mathrm{d}t} &= \Gamma^2_{00}u^0u^0 + 2\Gamma^2_{01}u^0u^1 + \Gamma^2_{11}u^1u^1 = 0 \\
\frac{\mathrm{d}u^3}{\mathrm{d}t} &= \Gamma^3_{00}u^0u^0 + 2\Gamma^3_{01}u^0u^1 + \Gamma^3_{11}u^1u^1 = 0
\end{aligned} \tag{3.3}$$

With the metric of Equation (3.1), we find that all the connection coefficients vanish in the first two of these equations. These equations just state that the corresponding velocity components are constant which they must be given that the metric is stationary. The LHS of the last two equations vanish because the velocity components are zero but in this case, the connection coefficients do not vanish. Working these out, we find,

$$\begin{aligned}
&c^2\left(u^0\right)^2 A^{(1,0)}[r,\psi] - \left(cu^1[r,\psi] - \omega[r,\psi]u^0\right) \\
&\times\left(cu^1[r,\psi]B^{(1,0)}[r,\psi] - u^0\left(\omega[r,\psi]B^{(1,0)}[r,\psi] + 2B[r,\psi]\omega^{(1,0)}[r,\psi]\right)\right) = 0 \\
&c^2\left(u^0\right)^2 A^{(0,1)}[r,\psi] - \left(cu^1[r,\psi] - \omega[r,\psi]u^0\right) \\
&\times\left(cu^1[r,\psi]B^{(0,1)}[r,\psi] - u^0\left(\omega[r,\psi]B^{(0,1)}[r,\psi] + 2B[r,\psi]\omega^{(0,1)}[r,\psi]\right)\right) = 0
\end{aligned} \tag{3.4}$$

Using the Milky Way as an example, the radius is around 4.7×10^{20} m and the rotation period of the outer regions is about 3×10^8 yrs $= 9.5\times10^{15}$ s which yields an angular velocity of $\omega = 6.6\times10^{-16}\,\mathrm{s}^{-1}$. The linear velocity at the outer edge of the galaxy is then about 3.1×10^5 ms^{-1} which is much less than the velocity of light despite the large radius. This fact allows us to assume that coordinate and proper time are the same sowe can approximate the 4-velocities as

$$u^{\mu}=\left(u^{0},u^{1},0,0\right)=\left(c,\dot{\varphi}_{vac}\left(r,\psi\right),0,0\right)$$
$$v^{\mu}=\left(v^{0},v^{1},0,0\right)=\left(c,\dot{\varphi}_{m}\left(r,\psi\right),0,0\right) \tag{3.5}$$

Since the angular velocities are very small, we expect these equations to be satisfied in the limit that ω and u^{1} vanish from which we have $A^{(1,0)}\left[r,\psi\right]=A^{(0,1)}\left[r,\psi\right]=0$

After eliminating the latter and replacing u^{0} and u^{1} using Equation (3.5), Equations (3.4) have the solution

$$\dot{\varphi}_{vac}\left(r,\psi\right)=\omega\left(r,\psi\right) \tag{3.6}$$

where $\omega\left(r,\psi\right)$ represents the overall rotation of the outer regions of the galaxy. The meaning of this is that the vacuum must rotate at a rate matching the observed rotation of the outer regions of the galaxy and we show in [2] that it does so with zero angular momentum. You will notice that there is no requirement for the rotating vacuum to have some minimal energy density. The fact of energy density is all that is required for this phenomenon to occur.

We now consider the stars whose velocity must also satisfy the corresponding set of geodetic equations. We separate their motion into a component that is at rest in the vacuum, and hence without angular momentum, and a residual with normal orbital motion. Thus, $\dot{\phi}_{m}=\dot{\phi}_{m,r}+\bar{\omega}$. Solving the equations gives

$$\dot{\phi}_{m,r}\left(r,z\right)=\frac{v}{r}-\bar{\omega}\left(r,z\right) \tag{3.7}$$

which exhibits the behavior shown in **Figure 7**. On the left is the normal orbital rotation, curve A, the first term on the right is the constant velocity component, curve B, and the second is the rigid body vacuum rotation, curve C. At the outer edge of the galaxy, the constant stellar velocity $v=\bar{\omega}\left(r_{G},0\right)$ equals the galaxy rotation rate so $\dot{\phi}_{m,r}\left(r_{G},0\right)=0$ which means that the *outermost stars are at rest in a rotating vacuum*.

In the new model, the vacuum was the structure, complete with rotation, that defined the material structure and within which the material came into existence. This explains why just the right amount of so-called dark matter always manages to accumulate just outside galaxies and why we don't find the galaxy here and there missing its dark matter halo. It even explains the opposite; galaxies without stars would be the result of an imprint for a galaxy that didn't contain the usual number of imprints for stars (empty bubbles.) The ordinary matter rotates with constant velocity because is it riding within a vacuum rotating as a rigid body.

To fully understand the dynamics of galaxies, it will be necessary to solve some version of Equations (3.1), and (3.2). What makes this problem difficult is that the effects we are interested in arise from the non-linearities within Einstein's equations. For example, inertial frame dragging is purely a relativistic effect. This means that the full set of equations must be solved without the use of simplifications such as linearization or even worse, by using Newton's laws. Doing so, however, is far beyond what can be done with a laptop computer and

we hope that someone with the necessary resources will eventually take on the problem.

We will now present a new solution to the gravitational lensing problem based on the interpretation of the curvature of spacetime as an index of refraction.

4. Galaxy Cluster Strong Gravitational Lensing

The idea behind the dark matter model of gravitational lensing goes back to the very beginnings of general relativity when Eddington measured the curvature of light from a star passing very close to the Sun to verify the prediction of Einstein's equations. Jumping to recent times, observers have been detecting single or multiple images of very distant sources such as quasars that result from their light rays being bent as they pass through galaxy clusters. Given the earlier success of Einstein's bending of light passing close to the Sun, it was natural to suppose that the same physics applied in other situations. There are many examples of lensing by galaxies [9], for example, and in those cases, because of their relatively high density and small size, Einstein bending is quite likely to be the dominant mechanism. In the galaxy cluster case, however, there was a problem because the amount of mass needed to achieve the observed angular deviations was about 10 times greater than the total baryonic mass of the clusters.

Unfortunately, when faced with the mass problem, instead of searching for a different mechanism to explain the bending, researchers filled the clusters with a huge amount of hypothetical, invisible dark matter. With enough mass, the magnitude of the bending can be made large enough to account for the observed images but at the same time, other problems arise such as reconciling the various methods for measuring the total mass of the clusters [10]. This, in turn, has led to additional constraints, such as the need for contrived distributions of the dark matter with a specific orientation relative to the line of sight to the Earth.

It is our contention the dark matter idea doesn't work and that the real solution to the problem lies in the variations in the vacuum curvature from one location to another across the cluster. Vacuum curvature slows the passage of light so in effect, it acts as an index of refraction. In **Figure 8**, we show the basic idea. Consider two light rays passing through some medium in which they experience different indices of refraction. The speed of any ray is given by c/n where n is the index of refraction so the ray with the smaller index of refraction will travel faster than the other. The result is a change in the propagation angle of the wavefront. During a time interval, Δt, photons will travel a distance $\Delta l_i = c\Delta t/n_i$ so $\tan(\Delta\alpha) = (\Delta l_2 - \Delta l_1)/R$, and since the angle is small, $\Delta\alpha \approx (1/n_2 - 1/n_1)(c\Delta t/R)$.

In **Figure 9**, we show a circle representing a galaxy cluster or a central portion of one together with an advancing path normal to the wavefront.

To do a proper analysis of this situation, we would need to define a profile for the index of refraction and then integrate it over each path to find the wavefront that develops. At this stage in our development, however, we are only interested in establishing that the refraction model is reasonable so we will be making a few

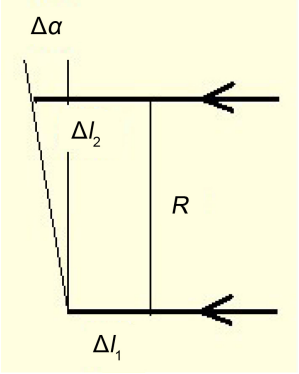

Figure 8. Refraction geometry.

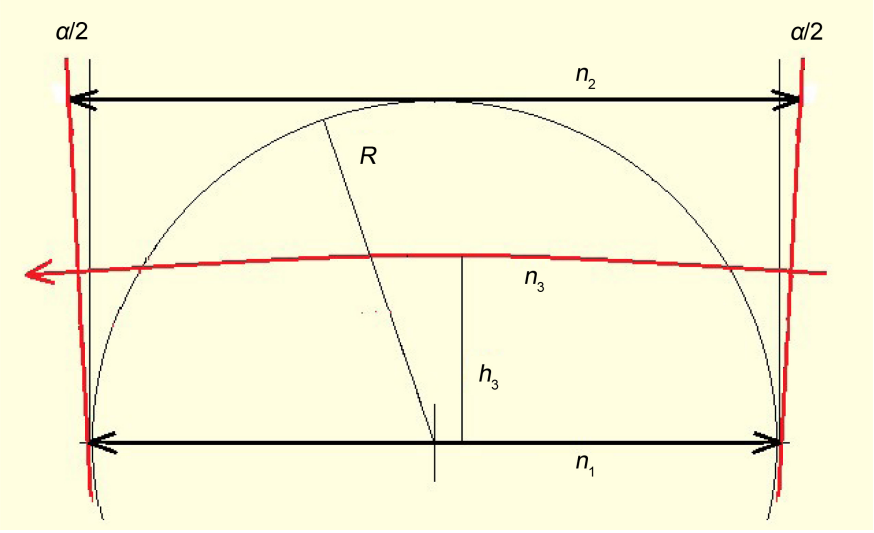

Figure 9. Galaxy cluster with advancing wavefront. The angle α is the refraction angle, n_i are the average indices of refraction at the indicated offsets from the center of the cluster, one of which is indicated by h_3. The parameter R is either the radius of the cluster or of some central portion of it.

approximations to simplify the work. In this case, we will assume an average index that is constant along each path. With that assumption, the refraction angle is given by

$$\alpha \approx \left(\frac{1}{n_3}-\frac{1}{n_1}\right)\frac{c\Delta t}{h_3} \tag{4.1}$$

Since $c\Delta t/n_1 = 2R$ we have

$$\alpha \approx \left(\frac{n_1}{n_3}-1\right)\frac{2R}{h_3} \tag{4.2}$$

If we next assume that the average index varies linearly with offset, $n(h) = n_1 - (h/R)(n_1 - n_2)$, we end up with

$$\alpha \approx 2\left(1-\frac{n_2}{n_1}\right) \tag{4.3}$$

for all paths crossing the cluster or the indicated portion of it. This, of course, is an oversimplification but it will be sufficient to establish the magnitude of the effects we wish to describe. With the assumption that the index of refraction decreases with distance from the center, the light rays bend towards the center which is the same sense as with the dark matter model.

We now need to make the connection with the vacuum curvature and to do this, we need to make another approximation. The issue is that the solution described in Section 2 is based on the idea of homogeneous and isotropic hyperspheres but now, we are considering regions that are neither since we are looking at a region of vacuum containing structures. To treat this properly, we would need to solve Einstein's equations with allowances made for the energy density of the vacuum imprint, and this we have not yet managed to do. Since the outcome must match the background result in the limit that the excess energy vanishes, we will proceed under the assumption that the correct metric will not be radically different from that of the background metric.

Starting with Equation (2.1), for photons $\mathrm{d}s = 0$ and if we fix our origin on the world line of a photon, we can set $\mathrm{d}\Omega = 0$. What remains is a quadratic equation which has the solution,

$$\frac{\mathrm{d}r}{\mathrm{d}t} = c\frac{\sqrt{1-k(t)r^2}}{a(t)F(t,r)}. \tag{4.4}$$

The definition of $F(t,r)$ is given in [2] and a plot of the background curvature is given in **Figure 5**. The proper distance the photon travels is $\mathrm{d}l(t) = a(t)\mathrm{d}r$ which leads us to the definition of the vacuum index of refraction,

$$\frac{\mathrm{d}l}{\mathrm{d}t} = c\frac{\sqrt{1-k(t)r^2}}{F(t,r)} \equiv \frac{c}{n} \tag{4.5}$$

Since $F(t,r)$ does not depend on the curvature,

$$n \propto \frac{1}{\sqrt{1-k(t)r^2}}. \tag{4.6}$$

This index of refraction increases rapidly as we travel back in time in part because the curvature is increasing but mostly because of the factor of r^2.

We now assume that the same formula is a reasonable approximation inside the cluster so,

$$\frac{n_2}{n_1} \approx \frac{\sqrt{1-k_1(t)r^2}}{\sqrt{1-k_2(t)r^2}} \tag{4.7}$$

From Equation (4.3), we know that the ratio is close to unity since the refraction angle is small so we can write $(n_2/n_1)^2 = (1-\alpha/2)^2 \approx 1-\alpha$ so

$$k_1 - k_2 \approx \frac{\alpha}{r^2} \tag{4.8}$$

which is the result we were after.

The reader will notice that we are saying that the curvature inside the cluster is greater than the background curvature which seems to contradict our earlier contention that the background curvature must be the maximum possible. The background solution, however, is based on the assumption of a homogeneous and isotropic universe whereas the interior of any structure is neither so the constraint doesn't apply.

We now turn to the full geometry which we show in Figure 10. To simplify the calculation, we assume that the source lies along the line of sight from the observer to the center of the cluster.

The angles θ and γ and the offset h can be expressed in terms of the refraction angle α,

$$\theta = \left(\frac{l_{cs}}{l_{oc} + l_{cs}} \right) \alpha , \tag{4.9a}$$

$$\gamma = \left(\frac{l_{oc}}{l_{oc} + l_{cs}} \right) \alpha , \tag{4.9b}$$

$$h = \left(\frac{l_{oc} l_{cs}}{l_{oc} + l_{cs}} \right) \alpha . \tag{4.9c}$$

Adding Equations (4.9a) and (4.9b) gives us the condition that

$$\alpha = \theta + \gamma . \tag{4.10}$$

The refraction angle is defined solely by conditions within the cluster and therefore has no dependence on the distances of either the source or the observer. The other two angles do vary with the distances for fixed values of the refraction angle. We obtain the distances by numerically integrating Equations (4.4) and (4.5) [2]. The redshift we obtain from its definition,

$$1 + z = \frac{\mathrm{d}r/\mathrm{d}t\big|_{t_s}}{\mathrm{d}r/\mathrm{d}t\big|_{t_o}} . \tag{4.11}$$

(We note that these give first principle results instead of values obtained from angular distance formulas which we have shown in [6] are only valid for small values of redshift.)

We are now ready to view some results. Our goal is to discover what constraints are placed on the curvature difference of Equation (4.8) by the observed lensing angles. Instead of using the difference directly, we use the normalized

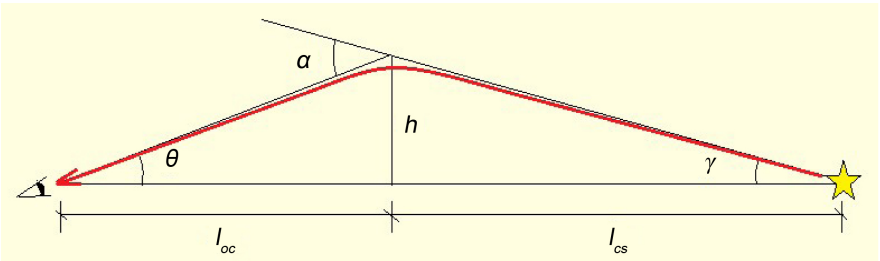

Figure 10. Lens geometry assuming the source lies along the line-of-sight of the observer.

difference defined by

$$K_{12} \equiv \frac{k_1 - k_2}{k_2} \tag{4.12}$$

as our independent variable because it is independent of time.

In Figure 11 and Figure 12, we show the observed, refraction, and source angles as a function of the redshift for three values of K_{12}. In Figure 11, the source redshift is $z_s = 1.5$, and in Figure 12 it is $z_s = 3.0$.

We find that the observed angle is sensitive to K_{12} and that the refraction and source angles are even more so. In Figure 13, we show the dependence of the angles on the *source* redshift for the single value $K_{12} = 0.015$.

Figure 13 shows only a single refraction angle curve which is a consequence of the fact that the refraction angle is independent of the source redshift. We also see that the observed angle shows much less sensitivity to the source redshift than it does to the cluster redshift. The reason for this is shown in Figure 14 where we see that l_{cs} becomes nearly independent of the redshift for values of source redshift greater than about 3.

We now want to compare these predictions with observation. Doing this in any detail would be a daunting task because one must allow for variations in the curvature throughout the cluster and also allow for the actual positions of the source or sources. Since we can't yet make such detailed maps of the curvature,

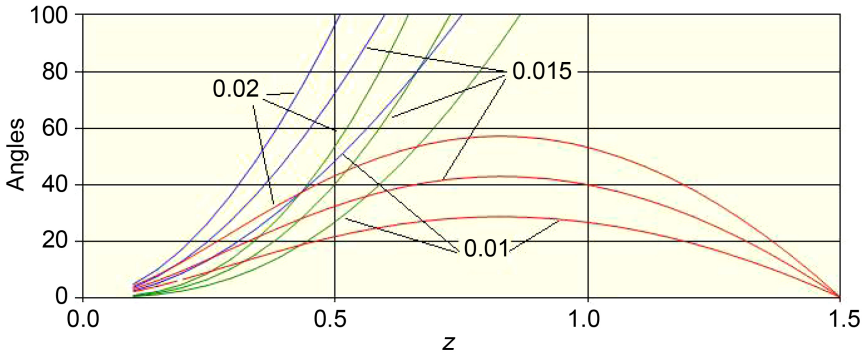

Figure 11. Observed (red). refraction (blue), and source (green) angles as functions of the cluster redshift for three values of K_{12} and a source redshift of $z_s = 1.5$.

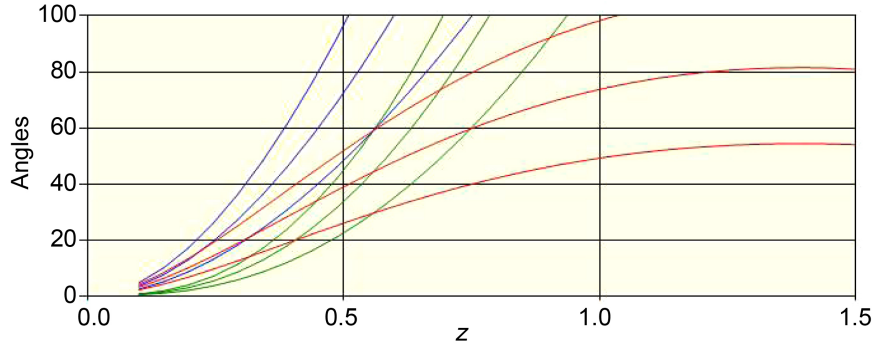

Figure 12. Same as Figure 11 except that the source redshift is $z_s = 3$.

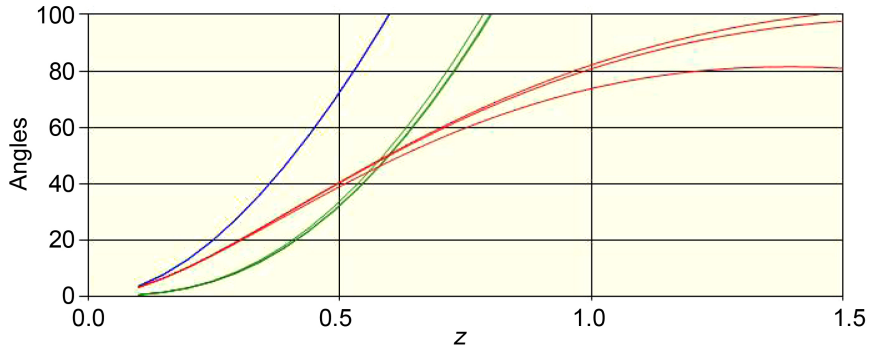

Figure 13. Variation of the observed, refraction, and source angles with the source redshift for a fixed curvature difference, $K_{12} = 0.015$.

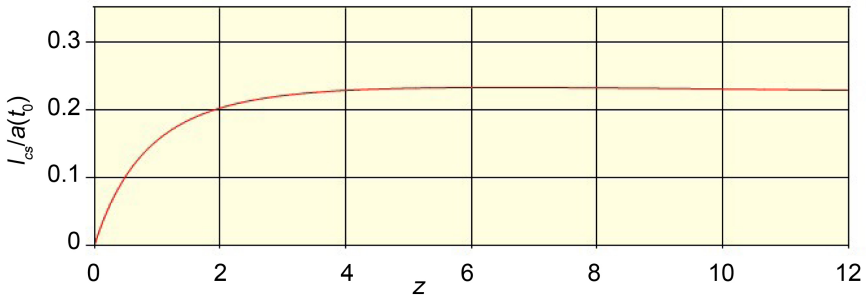

Figure 14. Cluster-Source path length as a function of source redshift.

we have taken a much more limited approach that is sufficient for making order-of-magnitude estimations.

Working from images presented in [10] [11] and [12] which show lensing within clusters with known redshifts, we estimated the magnitude of the largest refractions by simply measuring the offset of the images from the center of the cluster and then converting to an angle using the scales presented on the images. Choosing the image with the largest observed angle for each cluster gives the results shown in **Figure 15**. While there is a fair amount of scatter, the data do indicate a systematic dependence on the cluster redshift. We also show the model prediction for $K_{12} = 0.015$. This value is nothing more than an eyeball fit and while we could do a χ^2 fit, it would be pointless because our model involves too many approximations for the exact value to have any significance.

This dependence brings up another point. Each of the data points is an independent event (different clusters) so the fact that the points indicate a systematic dependence reminiscent of the Tully-Fisher relation could be taken as support for our new model of structure formation in which the formation was regulated by a vacuum imprint.

We now want to consider another issue that could eliminate the whole dark matter idea. In **Figure 16**, we again show the observed and refraction angle curves for $K_{12} = 0.015$.

These curves are predictions of the model but the relation between them is fixed by the geometric constraint, Equation (4.9a) which says that the refraction

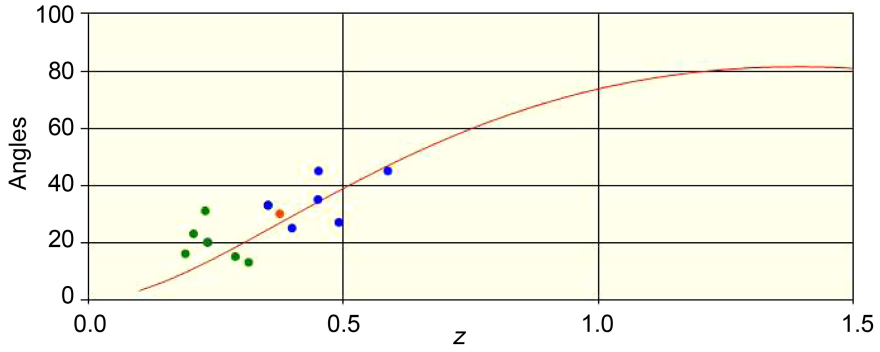

Figure 15. Magnitude of largest observed refraction as a function of redshift plotted against the predicted angle using a curvature difference of $K_{12} = 0.015$. The points in green are from [11], those in blue are from [12], and the single red point (Abell 370) is from [10].

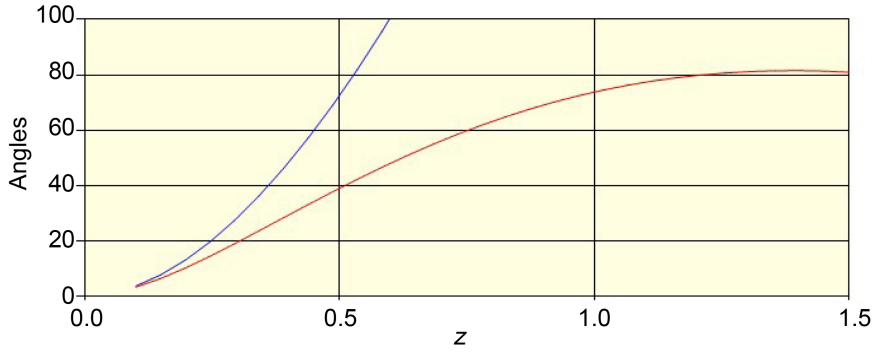

Figure 16. Observed and refraction angle curves for $K_{12} = 0.015$.

angle is always larger than the observation angle by a multiple determined by the ratio of path distances and further, that the divergence between the two curves increases rapidly with redshift. The point is that, because the data points match the predicted observation angle curve, the corresponding bending angle calculated using the dark matter model must match the indicated refraction angle curve. In the new model, the rapid increase in the refraction angle follows immediately from the r^2 dependence in Equation (4.8) but in the dark matter case, this same increase can only be achieved by an equally rapid increase in the amount of dark matter within the clusters since Einstein bending is proportional to the mass responsible for the bending. If the data trend continues out to a lens redshift of $z = 1.0$, for example, the amount of dark matter would have to be larger by a factor of about 3.5 than the value needed to explain the bending at $z = 0.5$. This would then mean that the dark matter content of clusters must be dissipating with time instead of remaining constant. Since no one is suggesting such a dissipation, if measurements at larger redshifts follow the trend, it will indicate a failure of the dark matter model.

5. Origin of the Curvature Gradient

We now have a good idea of how large the curvature difference must be to achieve

the observed refraction. The next step is to relate this to the curvature expected based on our new model of nucleosynthesis and cosmic structure formation.

We outlined the structure of our new model in the Introduction. In [4], we found that the initial vacuum energy excess needed to account for the creation of galaxy clusters was on the order of 2.5 and that the initial sizes of the proto-clusters were about 7 times their present-day sizes in present-day terms. (By that we mean that if one multiplies the size of a proto-cluster at the end of nucleosynthesis by the ratio of the scaling, $a(t_0)/a(t_{4000})$, the resulting size will be 7 times the present-day size of the cluster.) We further show in [5] that the matter energy density profile of the cluster must have a modest decreasing slope to achieve cluster stability at the time of galaxy formation.

Since the creation of matter involved only a very small percentage of the total vacuum energy, the initial vacuum energy over-density profiles would have continued to exist unchanged at least up until the time of galaxy formation because, as we show in [4], the expansion of the universe completely dominated the evolution up until then with gravitation having essentially no effect of the structures.

We now need to relate this initial vacuum energy density profile to the curvature difference needed to account for the cluster lensing. To make this connection, we will work with a toy vacuum energy density profile. We fix the parameters by imposing boundary conditions along with the requirement that the total mass of the vacuum over-density must be 2.5 times the mass of the same volume of background vacuum. For simplicity, we assume a cubic polynomial radial profile and spherical symmetry. For boundary conditions, we assume that the over-density vanishes at the outer boundary and that its derivative vanishes at both the center and at the outer boundary. The result is $\rho(l)=\rho_0\left(1-3(l/R_c)^2+2(l/R_c)^3\right)$ where $\rho_0=12.5$ and R_c is the radius of the cluster. In **Figure 17**, we show the result.

Beginning at a time of about $t\sim 4\times 10^{15}$ s, gravitation began to cause a contraction of the matter making up the proto-cluster which ended at a time of about $t_G\sim 1\times 10^{16}$ s when the clusters had reached their final, present-day size. Whether or not the vacuum also underwent contraction, we can't say at this time

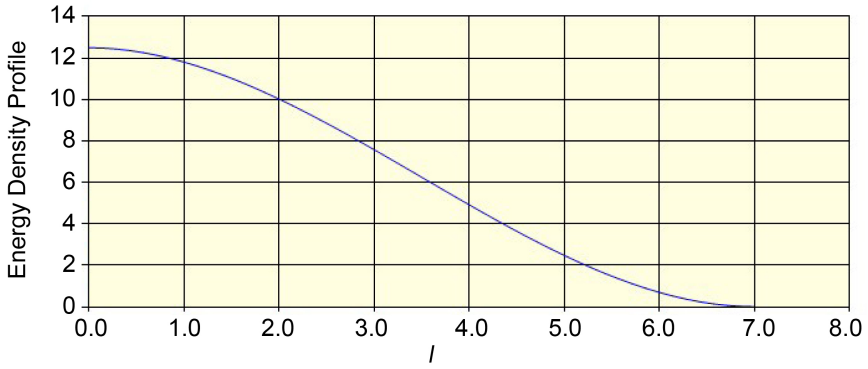

Figure 17. Toy vacuum energy density profile.

because we have not yet solved the full set of Einstein's equations for the evolution.

From Equation (2.7), we see that the curvature is proportional to the vacuum energy density so the curvature difference K_{12} is the same as the corresponding normalized vacuum energy difference. Assuming that the vacuum did not undergo contraction, the curvature difference is then $K_{12} = (\rho_0 - \rho_l)/\rho_l$ where ρ_l is the density evaluated at the distance l from the center of the cluster. If we evaluate the density at the outer boundary of the cluster, $l = R_{\text{cluster}}(t_0) = R/7$ and $K_{12} = 0.059$. If instead, we evaluate at the middle of the cluster, we have $K_{12} = 0.015$ which happens to agree with our earlier estimation of the required curvature difference. Strong lensing is generally thought to be associated with the core of the cluster which indicates that we should use an offset towards the center rather than at the outer boundary. If the vacuum did undergo contraction, it would increase the difference for a given offset.

The model presented so far assumes a uniform distribution of vacuum energy but from the scatter of the lensing data and the fact that the lensed images are sometimes arcs and at other times, single points, it is apparent that local variations in the index of refraction must be present. Such local variations, however, are also part of our imprint model of nucleosynthesis in which imprints contain sub-imprints. The imprint of the cluster regulated the creation of the cluster as a whole but it also contained sub-imprints that resulted in the creation of the galaxies within the cluster and within them, sub-sub-imprints that regulated the creation of the initial stars. For example, in [4] we showed that for large galaxies, the over-density was on the order of 17 and their size ratio was about 55. This means that the cluster vacuum was lumpy rather than smooth and this would lead to localized strong gradients of the index of refraction.

We find that our new model of nucleosynthesis together with our interpretation of the curvature of spacetime as an index of refraction can easily account for the bending of light needed to explain strong gravitational lensing. This shows that dark matter is not necessary to explain lensing and, if the observation angles continue to follow our predicted curve with increasing redshift, the dark matter model would not even be possible.

6. Conclusions

We start with the idea that the vacuum is characterized by its curvature which can vary from one location to another and that the vacuum carries energy which is manifested by its curvature. These are ideas with which most researchers will agree. That idea that ordinary matter derived from the vacuum will also not disturb too many people. Our final assertion is that the cosmological curvature varies with time. This is a new idea that runs counter to the prevailing view but there is no reason for the latter belief other than historic stubbornness. There is certainly no law of physics that says it must be constant and, as we have shown, the cosmological principle is no argument for a constant curvature either.

In this paper, we have shown that our new model based on those ideas alone can readily account for all the phenomena attributed to dark energy and dark matter. Invoking Occam's razor, we conclude that neither of them exists.

Conflicts of Interest

The author declares no conflicts of interest regarding the publication of this paper.

References

[1] Botke, J.C. (2023) Cosmology with Time-Varying Curvature—A Summary. https://www.intechopen.com/online-first/1167416

[2] Botke, J.C. (2020) *Journal of High Energy Physics, Gravitation and Cosmology*, **6**, 473-566. https://doi.org/10.4236/jhepgc.2020.63037

[3] Botke, J.C. (2022) *Journal of High Energy Physics, Gravitation and Cosmology*, **8**, 768-799. https://doi.org/10.4236/jhepgc.2022.83053

[4] Botke, J.C. (2021) *Journal of High Energy Physics, Gravitation and Cosmology*, **7**, 1373-1409. https://doi.org/10.4236/jhepgc.2021.74085

[5] Botke, J.C. (2022) *Journal of High Energy Physics, Gravitation and Cosmology*, **8**, 345-371. https://doi.org/10.4236/jhepgc.2022.82028

[6] Botke, J. C. (2023) *Journal of High Energy Physics, Gravitation and Cosmology*, **9**, 60-82. https://doi.org/10.4236/jhepgc.2023.91007

[7] Botke, J.C. (2021) *Journal of High Energy Physics, Gravitation and Cosmology*, **7**, 1410-1424. https://doi.org/10.4236/jhepgc.2021.74086

[8] Rubin, V. and Ford Jr., W.K. (1970) *The Astrophysical Journal*, **159**, 379. https://ui.adsabs.harvard.edu/abs/1970ApJ...159..379R/abstract https://doi.org/10.1086/150317

[9] Kochanek, C.S., Falco, E.E., Impey, C., Lehar, J., McLeod, B. and Rix, H.-W. *Castles Survey*. https://lweb.cfa.harvard.edu/castles/

[10] Kneib, J.-P. and Natarajan, P. (2011) *The Astronomy and Astrophysics Review*, **19**, Article Number 47. https://link.springer.com/article/10.1007/s00159-011-0047-3 https://doi.org/10.1007/s00159-011-0047-3

[11] Caminha, G.B., *et al.* (2019) *Astronomy and Astrophysics*, **632**, A36.

[12] Newman, A.B., Treu, T., Ellis, R.S. and Sand, D.J. (2013) *The Astrophysical Journal*, **765**, 24. https://iopscience.iop.org/article/10.1088/0004-637X/765/1/24/pdf https://doi.org/10.1088/0004-637X/765/1/24